Vendor-dependent mobile phase contaminants affect neutral lipid analysis in lipidomics protocols

Joshua A. Roberts[a], Angela S. Radnoff[a], Aleksandra Bushueva[a], Jocelyn A. Menard[a], Karl V. Wasslen[a,b], Meaghan Harley[a], Jeffrey M. Manthorpe[a,b], Jeffrey C. Smith[a,b,*]

[a] Department of Chemistry, Carleton University, Ottawa, ON, Canada

[b] Carleton Mass Spectrometry Centre, Carleton University, Ottawa, ON, Canada

* To whom correspondence should be addressed

Keywords: mass spectrometry, lipidomics, untargeted lipidomics, neutral lipids, contaminants, informatics, HPLC, LCMS-grade solvents

Corresponding author

* Email: jeff.smith@carleton.ca Phone: +1 613-520-2600 ext. 2408

Abstract

Lipidomics is a well-established field, enabled by modern liquid chromatography mass spectrometry (LCMS) technology, rapidly generating large amounts of data. Lipid extracts derived from biological samples are complex and most spectral features in LCMS lipidomics datasets remain unidentified, colloquially termed lipidomics “dark matter”. In-depth analyses of triacylglycerol, diacylglycerol, and cholesterol ester species revealed the expected ammoniated and sodiated ions as well as 5 additional higher mass dark matter peaks. These additional peaks were of relatively high intensity and resulted from analyte adduction with alkylated amine contaminants from LCMS-grade methanol and isopropanol. Tandem MS (MS/MS) of adduct peaks yielded no lipid structural information, producing only an intense ion of the adducted contaminant. Analysis of bovine liver extract identified 33 neutral lipids with an additional 73 alkyl amine adducts. Removing alcohols in place for acetonitrile and methyl *tert*-butyl ether in the mobile phase resulted in a 60% decrease in neutral lipid annotations, but eliminated the formation of alkyl amine adducts. Analysis of LCMS-grade methanol and isopropanol from different vendors revealed alkyl amine adduct formation in one out of three different brands that were tested. Substituting solvents increased lipid annotations by 36.5% or 27.4%, depending on the vendor and resulted in >2.5-fold increases in peak area for neutral lipid species, dramatically affecting their quantification and detection. Using principal component analysis, the same bovine liver sample separated into vendor-based clusters. These findings demonstrate the importance of solvent selection and disclosure during lipidomics protocols and highlight the challenges when comparing data between experiments.

Introduction

Lipidomics is a growing field that aims to characterize the complete set of all lipids in a biological matrix[1]. Lipids are a diverse group of biomolecules and serve a wide variety of functions in living organisms. The LIPID MAPS Structure Database[2,3] represents the largest repository of lipid structures, housing 48,205 structures as of 2023, both from curated and computationally generated sources. Glycerophospholipids and sphingolipids are commonly associated with membrane structure, lipid-protein interactions and cell signaling events[4]. Neutral lipid classes, such as triacylglycerols (TG), diacylglycerols (DG) and cholesterol esters (CE) have critical roles in energy metabolism, membrane fluidity regulation and signaling pathways[5]. Liquid chromatography mass spectrometry (LCMS) platforms are the primary tool for lipidomics applications, due to their sensitivity, qualitative and quantitative data insights and high-throughput capabilities[6]. Lipidomics has been applied to study numerous health conditions and disease models[7–9], providing insight to researchers and clinicians.

Accompanying any lipidomics dataset is a large group of unidentified spectral features that are generated by untargeted LCMS workflows and modern data preprocessing software, often termed lipidomics "dark matter"[10]. This is also encountered in the proteomics[11] and metabolomics[12] fields. Elucidating the identity of dark matter is often associated with database expansion or the incorporation of orthogonal separation techniques, such as ion mobility[10,13]. Identifying the proportion of dark matter that is related to the biological material in the sample, such as novel biomolecules, is difficult to determine, as matrix contaminants, data artifacts and in-source fragments are frequently encountered in LCMS platforms utilizing electrospray ionization[14,15]. It has been estimated

that 98% of spectral features in omics datasets may be dark matter[12]. Due to these factors, characterization of lipidomics dark matter remains a major challenge for the field moving forward.

A recent publication by Cajka et al.[16] highlighted that quality variation in LCMS-grade solvents has been overlooked in the field and provided an assessment of isopropanol from 5 different vendors. Their results show a wide range of background signal intensities in the low-mass region. The isopropanol from some vendors produced enough background signal to suppress the maximum total ion current intensity from a human serum extract up to 60% compared to other vendors. Furthermore, they and others[17,18] observe neutral lipid classes adducting to protonated ethylamine, originating from acetonitrile reduction during electrospray ionization, forming $[M+46]^+$ ions in both commercial standards and complex biological extracts. Alkylated amines have been previously added to LC mobile phases to enhance the ionization of different analytes including anabolic agents[19], hydroperoxyoleates[20] and polymers[21]. As discussed herein, preliminary tests on commercial standards revealed a complex pattern of 4 unknown adduct peaks beyond the commonly observed $[M+NH_4]^+$, $[M+Na]^+$, $[M+K]^+$ peaks and the previously observed $[M+46]^+$ ion. The four novel adducts were all of higher mass and suspected to be contaminants found in the LCMS-grade solvents used as mobile phases. Methanol and isopropanol were determined to be the source of these alkylated amine species, prompting a thorough investigation into vendor-based differences in LCMS-grade solvents and the impacts they have on lipidomics dataset acquisition, processing, and ultimately the quality of the results reported.

Experimental Section

Materials and Reagents: LCMS-grade water (Omnisolv LCMS), ammonium formate, ammonium fluoride, ammonium bicarbonate, ammonium acetate, *N*-methyl-*p*-toluenesulfonamide and tetrafluoroboric acid diethyl ether complex were purchased from Millipore Sigma (St. Louis, United States). Optima LCMS-grade acetonitrile, HPLC-grade methyl *tert*-butyl ether and diethyl ether were purchased from Fisher Scientific (Waltham, United States). LCMS-grade methanol and isopropanol were purchased from Honeywell (Chromasolv LCMS, Morris Plains, United States), Sigma (Hypergrade LCMS LiChrosolv) and Fisher Scientific (Optima LCMS). Vendor names are randomized and not directly named in the text for confidentiality. Toluene, chloroform and KOH were purchased from Caledon Laboratories Ltd. (Georgetown, Canada). Glass centrifuge tubes were purchased from Kimble (Vineland, United States). TG 15:0-18:1-d_7-15:0, DG 16:0-18:1, CE 17:0, PG 16:0-18:1 and PA 16:0-18:1 were purchased from Avanti Polar Lipids (Alabaster, AL, United States). Absolute ethanol was purchased from Commercial Alcohols Inc. (Brampton, ON, Canada).

Sample Preparation: 50 mg of bovine liver was thawed and extracted using a modified Bligh-Dyer method[22,23]. Briefly, liver was transferred to conical 10 mL glass centrifuge tubes. 1 mL of water with 0.1 M sodium acetate and 2 mL of methanol with 2% acetic acid (v/v) were added to each tube and then homogenized by hand and bath sonicated for 5 min. 1.5 mL of chloroform was then added to each tube and shaken for 2 min, then centrifuged (528 × g, 2 min). The chloroform layer was carefully removed by Pasteur pipette and transferred to a new 10 mL glass centrifuge tube. The water/methanol layer was then extracted two more times with 1 mL of chloroform with each chloroform layer

combined with the previous extractions for a total of 3.5 mL per sample. The chloroform was then evaporated under a stream of nitrogen gas and dissolved in 1 mL of ethanol and incubated at 30°C for 10 min, centrifuged (528 g, 2 min) and transferred to an Agilent amber HPLC vial with a Polytetrafluoroethylene-lined cap. All lipid standards were prepared at either 10 or 1 µM in toluene. Diazomethane was synthesized from *N*-methyl-*N*-nitroso-*p*-toluenesulfonamide as previously described[24,25]. Lipid solutions of PG and PA were derivatized in-solution as previously reported using the trimethylation enhancement using diazomethane (TrEnDi) method[26].

LCMS analysis and Data Processing: All data were acquired using an Agilent 6546 QToF mass spectrometer operating in positive polarity with an Agilent 1260 LC system using MassHunter Acquisition Software (version 10.0). Separation via HPLC was achieved using an Agilent Poroshell 120 EC-C_{18} (2.7 um, 2.1x100 mm) for alcohol-based methods or a Thermo Scientific BioBasic-4 (5 µm, 150x4.6 mm) for methyl *tert*-butyl ether-based methods. Flow injection analysis was also performed for selected experiments by removing the chromatography column and connecting the HPLC effluent directly to the mass spectrometer. The column compartment was heated to 45^{o}C and injection volumes of 5 µL for on-column or 10 µL for flow injection analysis with a flow rate of 400 µL/min used for all analyses. The following source parameters were used for all analysis, gas temp 200°C, drying gas 10 L/min, nebulizer 50 psi, sheath gas temp 300°C, sheath gas flow 12 L/min, VCap 3500 V, fragmentor 150 V, skimmer 75 V, Oct 1 RF Vpp 750 V, mass range of *m/z* 40–1700 and an acquisition rate of 3 spectra/s. A data-dependent MS/MS acquisition method was used with the following settings: quadrupole isolation width of 1.3 *m/z*, 10 precursors/cycle, absolute threshold 5000 counts, active exclusion enabled after

1 spectrum and released after 0.15 min, abundance dependent accumulation of 25,000 counts/spectrum, purity stringency of 70% and a purity cut-off of 0%. A triplicate of TG 15:0-18:1-d_7-15:0 (10 µM in toluene) was also acquired using a Sciex QTrap 4000 coupled to a Dionex Ultimate 3000 using an Agilent C_{18} Poroshell 300SB-C_{18} (5 µm, 75 x 2.1 mm) column. Mobile phases consisted of water, acetonitrile, methyl *tert*-butyl ether, methanol or isopropanol in compositions that are specified where relevant in the text. LCMS-grade alcohols were compared between each vendor using bovine liver extract and commercial standards; solvent A consisted of 50:50 water and methanol with 10 mM ammonium formate, solvent B consisted of 25:75 methanol and isopropanol with 10 mM ammonium formate. The following HPLC gradient program was used: 0 min 20% B, 0.5 min 20% B, 10 min 100% B, 20 min, 100% B followed by 5 min of re-equilibration at the gradient's starting conditions. To clean and condition the LCMS system when comparing solvents from different vendors, a 1:1 mixture of water and acetonitrile was flushed through the hydraulic path and column for 10 min, followed by 60 min of washing with the vendors solvents at a 1:1 mixture of solvent A and B. In addition, two no-injection blanks were conducted prior to the analysis of lipid standards or bovine liver extract samples to ensure no sample carryover. For HPLC gradients using methyl *tert*-butyl ether, solvent A was water with 10 mM ammonium formate, while solvent B was 10:60:30 water, acetonitrile and methyl *tert*-butyl ether with 10 mM ammonium formate. The HPLC gradient program was 0 min 40% B, 0.5 min 40% B, 10 min 100% B, 40 min, 100% B. Data were analyzed using Agilent MassHunter Qualitative Analysis (version 10.0) or converted to .mzML format using Proteowizard's MSConvert[27] and imported into MzMine[28] (version 3.3.0). Agilent Lipid Annotator was used for all lipid identifications using

the default method. Microsoft Excel and R were used for plotting and filtering data. Lipid features were extracted using the “Targeted Feature Detection” module in MzMine. Peak areas were then normalized by $\log_2$ transformation and batch corrected using the Limma package (version 3.44.0) in R.

Results and Discussion

Neutral lipids are best identified in LCMS workflows as ammonium adducts[29–31], as they produce the most informative fragmentation patterns. Consequently, volatile ammonium salts, such as ammonium formate or ammonium acetate, are commonly added to mobile phases to promote ammonium adduct formation while also improving chromatographic performance[32]. Reversed phase chromatography schemes consisting of various proportions of water, methanol, acetonitrile and isopropanol are employed to separate lipid classes by acyl-chain length and degree of unsaturation[6]. A recent publication by Cajka et al.[16] investigated vendor-based contamination in isopropanol, demonstrating the effect of solvent vendor in lipidomic profiling experiments, with some vendors generating large amounts of background signal and ultimately lowering sensitivity for orbitrap-based instruments. They also showed that ethylamine contaminants originating from acetonitrile can adduct to TG species, complicating lipidomic profiling of complex samples. Our observations corroborate these results while also adding a considerable amount of depth regarding the deleterious effects that solvent contamination can have on the identification and quantification of neutral lipids.

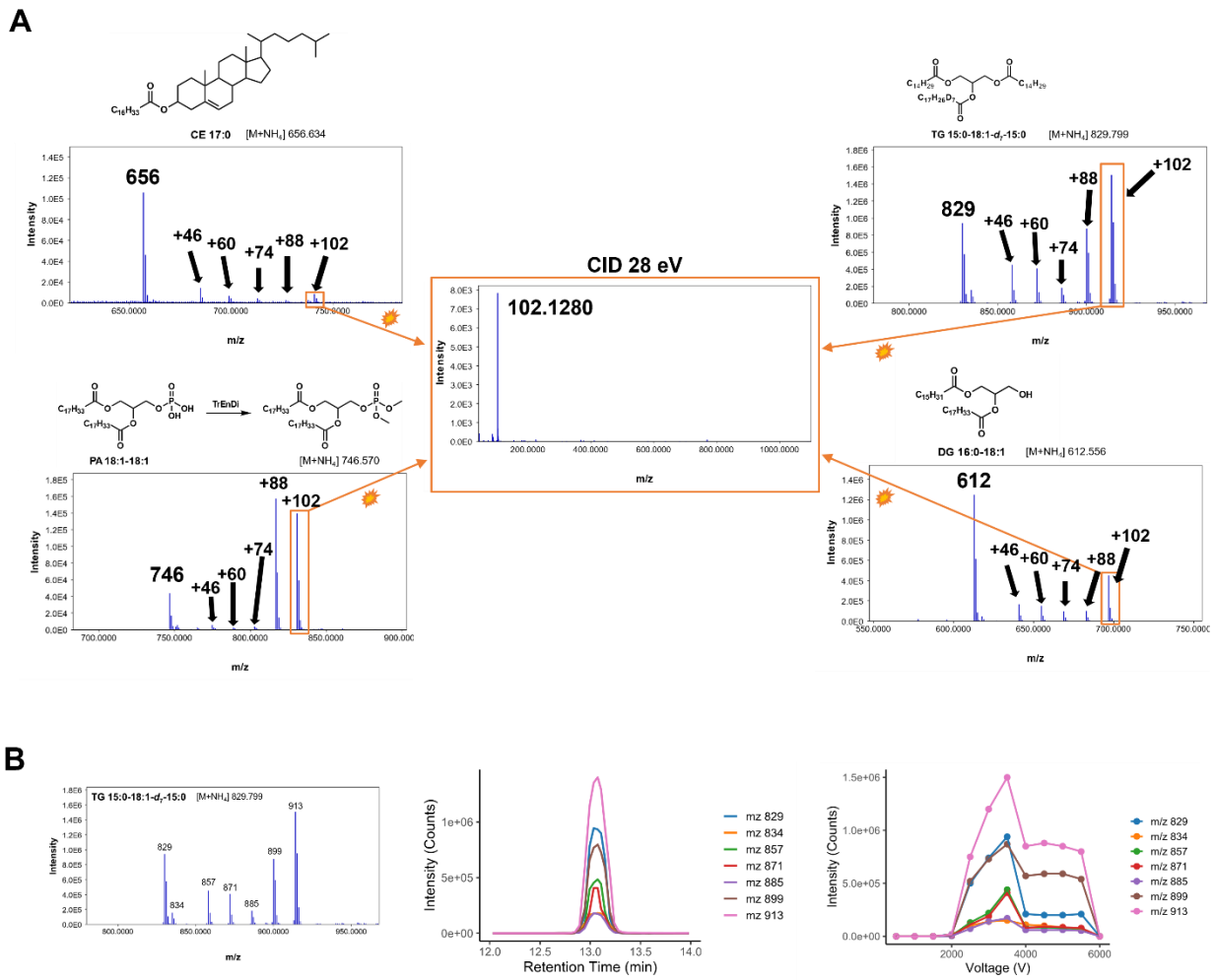

Figure 1. Unknown adducts provide charge to major neutral lipid standards in LCMS analysis. A) MS-level scans of CE 17:0, DG 16:0-18:1, TG 15:0-18:1-d_7-15:0 (all at 10 μM) and permethylated PA 16:0-18:1 (1 μM) derivatized by TrEnDi, eluted using a binary LC gradient of water, methanol and isopropanol with 10 mM ammonium formate. Additional peaks appear with *m/z* offsets of 46, 60, 74, 88 and 102 from the lipid species exact mass and are the primary MS/MS peaks present after CID. B) All adduct masses of TG 15:0-18:1-d_7-15:0 (spectra with *m/z* included) elute from the LC at the same time, suggesting they are from the same lipid species. Adducts also appear at a wide range of ESI voltages.

Analysis of commercially available DG, TG and CE standards revealed a complex and reproducible pattern of peaks in addition to the $[M+NH_4]^+$ and $[M+Na]^+$ adducts that are typically observed for these lipid classes (Figure 1A). CID of these peaks at 28 eV

produced MS/MS spectra that had a single intense peak corresponding to the *m/z* difference between the parent mass and the standard's neutral exact mass, either by 46, 60, 74, 88 or 102 (Supporting Figure S1). For all standards that were analyzed, all of the additional *m/z* features elute at the same time and also appear in similar abundance ratios across a wide range of ESI voltages, suggesting that these are all adducts of the same lipid standard (Figure 1B). Furthermore, this phenomenon was observed across instrument platforms that have different ESI source architecture (Supporting Figure S4) and on similar Agilent instrument platform, but in a different laboratory (data not shown). Previous findings identify an ethylamine adduct ($[M+46]^+$)[17] and observed its interaction with TG species[18], as well as DG and CE species[32]. To our knowledge, this is the first report of higher mass adducts of this nature. Analysis of other common phospholipid species, such as phosphatidylcholine and phosphatidylethanolamine species did not produce the same pattern of higher mass peaks. Phosphatidic acid (PA) and phosphatidylglycerol (PG) standards were observed to form additional $[M+88]^+$ and $[M+102]^+$ species at 0.33-fold and 0.62-fold intensity relative to their typical $[M+NH_4]^+$ ions, respectively. PA and PG species modified using Trimethylation Enhancement using Diazomethane (TrEnDi)[25,26] to produce permethylated neutral lipids that form ammoniated ($[M^{Tr}+NH_4]^+$) ions[33] also formed $[M+88]^+$ and $[M+102]^+$ species, but at much greater intensity relative to the $[M^{Tr}+NH_4]^+$ peaks (3.28-fold and 5.44-fold, for PA and PG, respectively) than unmodified PA and PG (Supporting Figure S2 and S3).

Table 1. Measured adduct *m/z* in the ESI low-mass region and their molecular formulas calculated using MassHunter Qualitative Analysis (version 10.0). The mobile phase consists of methanol (25%) and isopropanol (75%) with 10 mM ammonium formate. Observed *m/z* and peak heights are averaged over 1 min of analysis time at a flow rate of 400 µL/min.

Observed *m/z* $[M+H]^+$	Calculated Ion Formula	Error (ppm)	Theoretical *m/z* $[M+H]^+$	Peak Height (Counts)
102.1279	$C_6H_{15}NH$	1.72	102.1277	1.3E6
88.1120	$C_5H_{13}NH$	-0.87	88.1121	4.4E5
74.0965	$C_4H_{11}NH$	1.02	74.0964	3.8E2
60.0805	C_3H_9NH	-4.67	60.0808	4.0E3
46.0650	C_2H_7NH	-2.79	46.0651	1.0E4

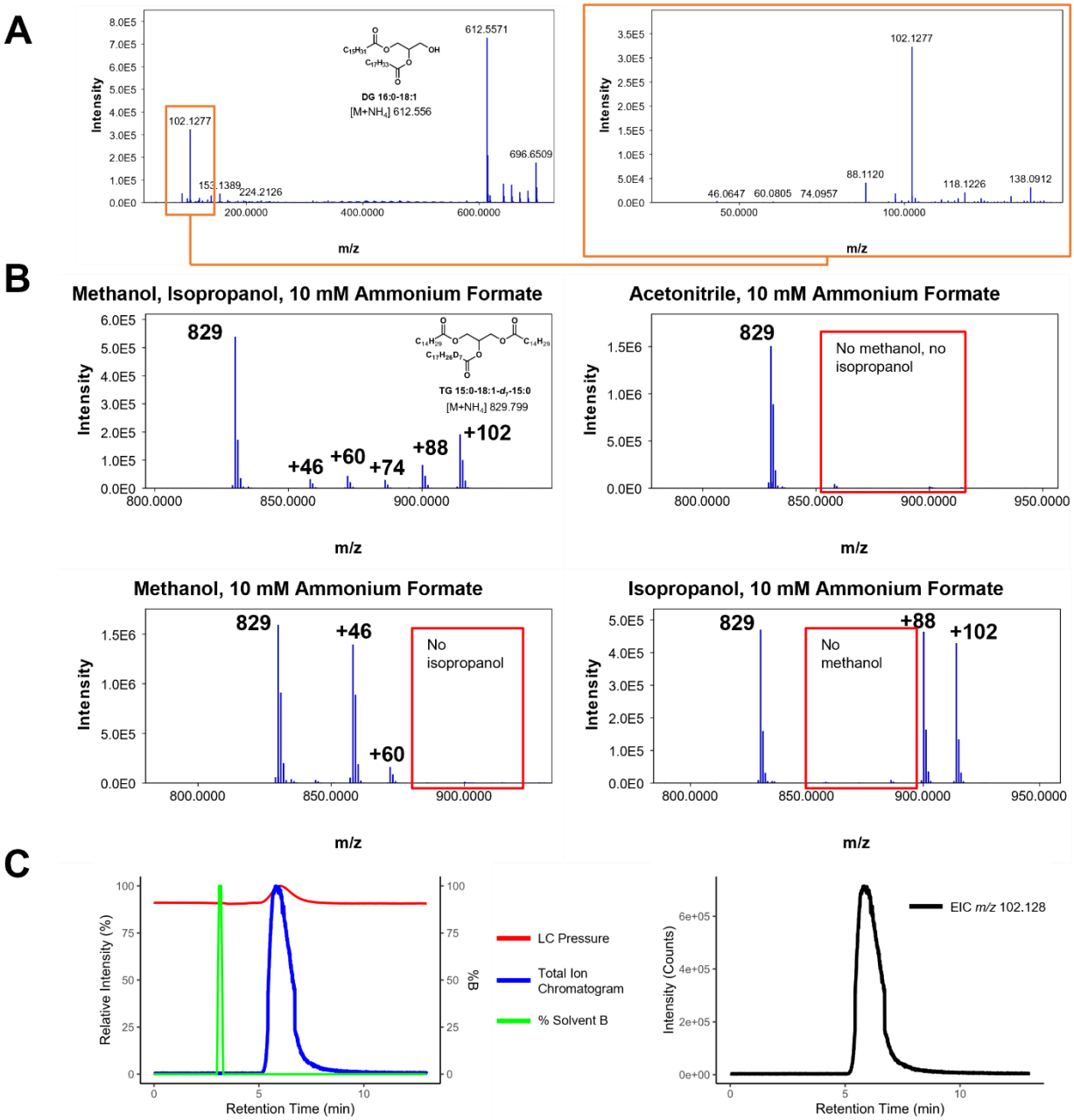

Figure 2. Adducting *m/z* are found in the low-mass region of ESI spectra when using a mobile phase of water, methanol and isopropanol with 10 mM ammonium formate. A) Additional adduct peaks are observed for DG 16:0-18:1, examining the low-mass region (highlighted in orange) shows the same *m/z*. B) Flow injection analysis of TG 15:0-18:1-d_7-15:0 with different mobile phases show different adduct patterns. Methanol (25%) and isopropanol (75%) with 10 mM ammonium formate shows all observed adducts. Eliminating both alcohols from the mobile phase and using only acetonitrile with ammonium formate produces only the TG ammonium adduct. Methanol and isopropanol in isolation contain different contaminants that adduct to TG 15:0-18:1-d_7-15:0, only *m/z* 46 and 60 appear in methanol, while *m/z* 88 and 102 appear in isopropanol. C) Using a mobile phase of 50% water and 50% acetonitrile as solvent A

produces a low and constant total ion chromatogram (TIC) signal. When the mobile phase is abruptly changed to 100% solvent B (water (5%), methanol (27.5%) and isopropanol (67.5%) with 10 mM ammonium formate) for 0.1 min and then returned to 100% solvent A, a large increase in TIC signal is observed corresponding with a change in the LC pressure. Most of this signal increase corresponds to *m/z* 102.128, indicated by the extracted ion chromatogram (EIC) on the right.

It was noted that all of the *m/z* values corresponding to these adducts were observed in the low-mass region of the MS-level spectra and were suspected to be solvent contaminants (Table 1 and Figure 2A). All adducts were proposed to be alkylated amine structures, based on their predicted elemental compositions calculated from their accurate masses, and their intensities spanned 3 orders of magnitude. Cajka et al.[16] identified the higher mass portion (*m/z* 88, 102 and 116) of this homologous series of amines as mobile phase impurities. In the analysis herein, *m/z* 116 was observed in the low-mass region of the MS-level scans, but was not found to adduct with any neutral lipid species in our data. To test which solvents were producing these peaks, a commercial TG standard was analyzed by flow injection analysis in acetonitrile, methanol and isopropanol, each with 10 mM ammonium formate. Solvents were analyzed individually and compared to 25% methanol and 75% isopropanol, which is the approximate mobile phase composition that these adduct species were initially identified using a binary HPLC gradient (Figure 2B). When both methanol and isopropanol are used as the mobile phase, all adduct *m/z* are observed. However, only *m/z* 46 and 60 adducts appear with 100% methanol, while only *m/z* 88 and 102 were observed in 100% isopropanol. Using acetonitrile eliminated all alkylated amine adducts and produced a $[M+NH_4]^+$ peak with a 3-fold increase in intensity compared to the original 25:75 methanol and isopropanol mixture. This is contradictory to previous findings specifically linking the ethylamine (*m/z*

46) adduct as a reduction product of acetonitrile and water during electrospray[16–18]. Other nitrogen-containing adduct species with neutral lipids, such as acetamidinium ($[M+C_2H_6N_2+H]^+$) produced from acetonitrile, have previously been reported[34], but were not observed using acetonitrile under the current conditions. To confirm that the LCMS-grade alcohols were the source of the alkylated amines, a 50:50 mixture of water and acetonitrile was held constant, producing a low-intensity and constant total ion chromatogram (TIC, Figure 2C). The mobile phase was abruptly switched to water (5%), methanol (27.5%) and isopropanol (67.5%) with 10 mM ammonium formate for 0.1 min. A pressure change was noted approximately 3 min later, signaling that the combination of methanol and isopropanol was eluting from the HPLC, and a large increase in total ion current was observed. An extracted ion chromatogram (EIC) showed that this TIC peak coincided with an increase in *m/z* of 102.128, which is the dominant alkylated amine adduct. Altering the type of ammonium salt did not affect the appearance of these alkylated amines (Supporting Figure S5), further suggesting that they are contaminants in the LCMS-grade products. CID analysis of *m/z* 102.128 was compared to diisopropylamine, which has the same molecular formula calculated for 102.128 (Supporting Figure S6). Analysis of the MS/MS spectra showed several shared fragment ions with the unknown *m/z* 102 adduct. However, additional peaks with *m/z* of 46, 57 and 72 were also present in the contaminant *m/z* 102 MS/MS spectra, suggesting the contaminant adduct may be a mixture of $C_6H_{15}N$ isomers.

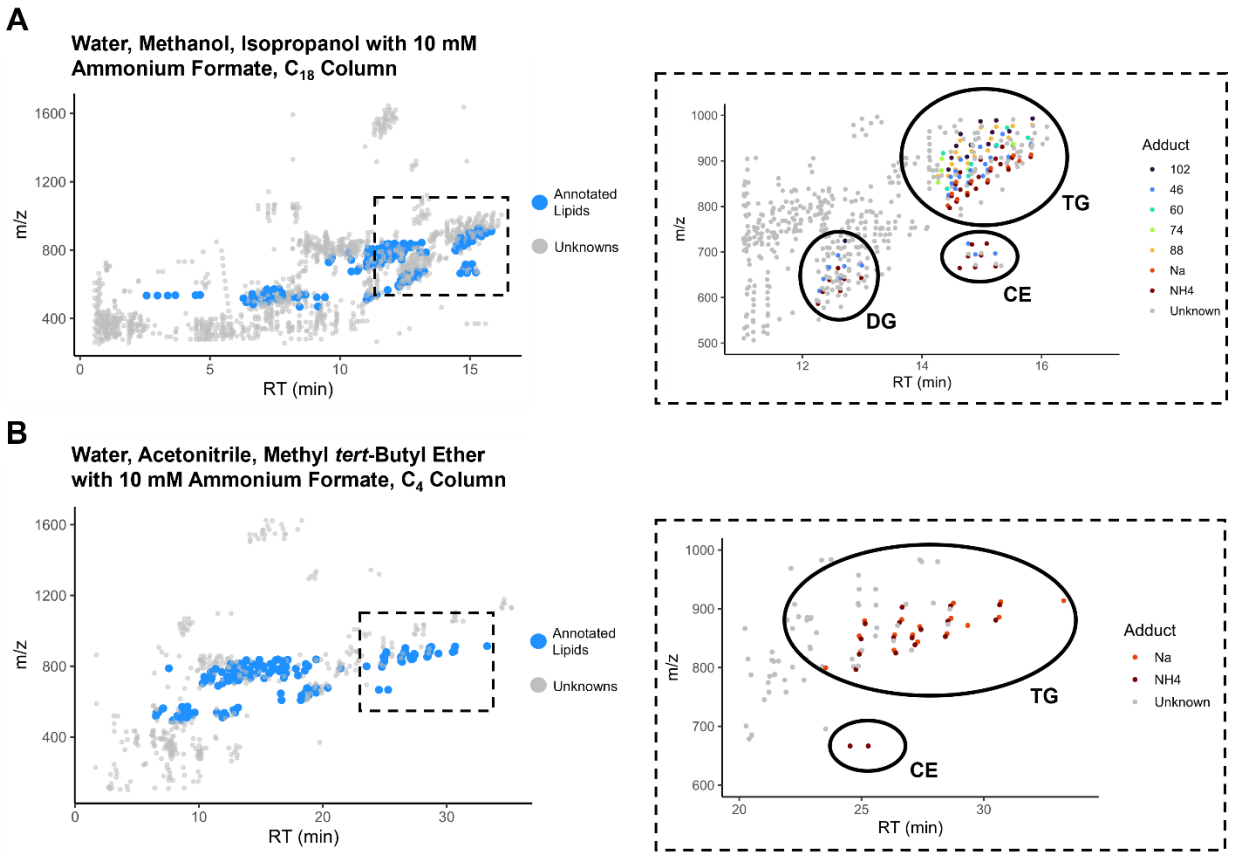

Figure 3. LC gradients consisting of methanol and isopropanol generate large amounts of dark matter associated with neutral lipids in bovine liver lipid extract A) Using a binary gradient consisting of water, methanol and isopropanol with 10 mM ammonium formate, 33 neutral lipids were detected, but large amounts of alkylated ammonium adducts were also observed. B) An alcohol-free mobile phase consisting of water, acetonitrile and methyl *tert*-butyl ether with 10 mM ammonium formate removes the presence of alkylated ammonium adducts and results in 20 neutral lipid annotations.

To determine the impact that the alkylated amine contaminants had on a complex lipidomics sample, bovine liver extract was analyzed in positive polarity using a binary HPLC gradient. Mobile phase A was 50:50 water and methanol and mobile phase B consisted of 25:75 methanol and isopropanol, both contained 10 mM ammonium formate. Over a linear 20 min gradient, 174 lipids were annotated using Lipid Annotator from 1545 total features (Figure 3A). 33 neutral lipid species from the TG (n=19), CE (n=7) and DG

(n=7) classes were identified. Each DG species and 3 of 7 CE species that were annotated had a corresponding *m/z* 46 adduct (Supporting Table S1). TG species were the most affected neutral lipid class, producing an additional 59 features from the 19 identities corresponding to alkylated amine adducts, representing an increase of 310% TG-associated peaks. The *m/z* 46 adduct was identified for each annotated TG in the dataset, with *m/z* 88 being the next most common affecting 89% of TG species. The *m/z* 74 adduct was the least common, only associating with 5 of all identified TG species. The *m/z* 102 adduct, which was most abundant when examining commercial standards of TG and DG species, was only identified for 12 of the 19 TG species (63%) in the sample. The *m/z* 60 adduct was only identified for 6 of the 19 TG species (21%). As acetonitrile was shown to eliminate alkylated amine adduct formation by flow injection analysis, the same sample of bovine liver extract was analyzed using a binary HPLC gradient without methanol or isopropanol (Figure 3B). Acetonitrile alone, though, is not a practical option for LCMS-based lipidomics due to its low eluent strength and the strong interactions between neutral lipid species and reversed-phased columns. As a result, solvent B was made to a ratio of 10:60:30 water, acetonitrile, and methyl *tert*-butyl ether to increase the elution strength of solvent B, while solvent A was water. Both solvents A and B contained ammonium formate at a concentration of 10 mM. Methyl *tert*-butyl ether has compatibility issues with some HPLC components, thus was kept to a 30% maximum concentration, as recommended by the LC manufacturer, while 10% water was required to solubilize 10 mM ammonium formate in solvent B. To elute CE and TG species under these conditions, a C_4 column was employed for the analysis. While no alkylated amine adducts were detected for CE and TG species, only 20 neutral lipid species were identified (Supporting

Table S2) as compared to 33 using water, methanol and isopropanol. No DG species were annotated in the sample using this method. Chromatographic performance suffered due to the high proportion of methyl *tert*-butyl ether in the mobile phase and the high ratio of water required to solubilize ammonium formate (Supporting Figure S7). While chromatographic peak shape is improved using methanol and isopropanol with a C_{18} HPLC column, the *m/z* 46 adduct creates an isobaric peak with TG species possessing acyl chains containing 2 additional carbons, creating a XIC doublet for each $[M+MH_4]^+$ TG peak (Supporting Figure S7). This has been shown previously by Cajka et al.[16] and adds additional complexity to the analysis of neutral lipids when alkylated amine adducts begin forming. These results demonstrate that methanol and isopropanol remain the ideal solvents for lipidomics applications, the latter of which being the most essential and widely used in the field. Thus, improving our understanding of methanol and isopropanol contamination and how it affects complex lipidomics samples, is critical to ensuring high-quality and consistent results.

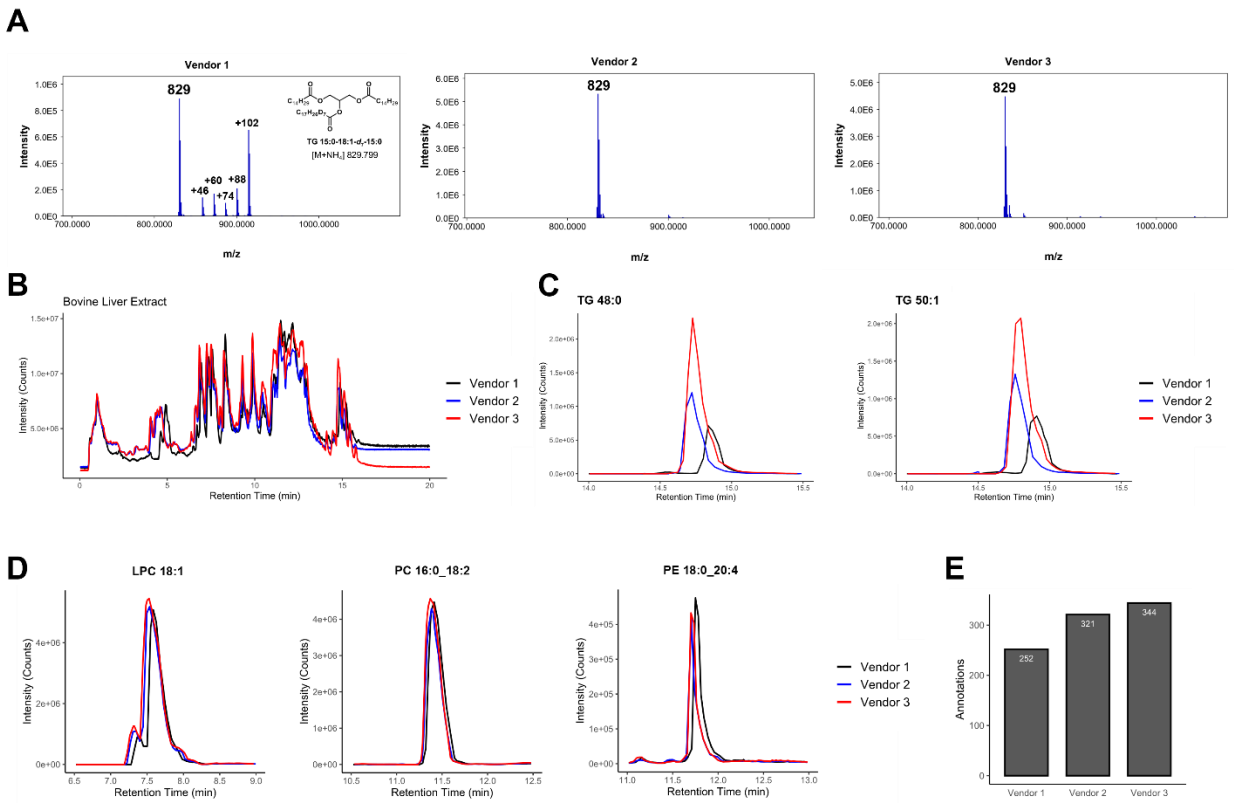

Figure 4. Using LCMS-grade methanol and isopropanol from different vendors alters alkylated ammonium adduct formation and dramatically changes neutral lipid analysis. A) TG 15:0-18:1-d_7-15:0 eluted on a binary gradient of water, methanol and isopropanol with 10 mM ammonium formate. Methanol and isopropanol purchased from 3 different vendors are compared, water and ammonium formate are from the same vendor in each trial. Analysis from Vendor 1 produces the adducting pattern previously observed with neutral lipids, while Vendors 2 and 3 only produce ammoniated and sodiated adducts. B) The same sample of bovine liver lipid extract is analyzed with alcohols from all 3 vendors. C) Abundant TG species show dramatic differences in intensity when compared between vendors. D) Other major classes of phospholipids are unaffected. E) A 36.5% increase in lipid annotations is observed comparing the same sample from Vendor 1 to Vendor 3, a 27.4% increase was found when switching from Vendor 1 to Vendor 2.

To investigate the impact of the vendor-based differences in LCMS-grade solvent quality have on neutral lipid analysis, methanol and isopropanol from an additional 2 vendors were purchased and compared using TG 15:0-18:1-d_7-15:0 (Figure 4A). Vendor

1 was used exclusively in data shown until Vendors 2 and 3 were purchased. Vendors 2 and 3 showed no alkylated amine TG adducts and resulted in a 5.96-fold sensitivity enhancement for the same 10 μM TG standard comparing vendors 2 to 1. A 5.06-fold increase was observed comparing vendors 3 to 1. Using the same sample of bovine liver extract, each vendor was also compared and differences in the TICs are observable in baseline noise level and at various retention time points (Figure 4B). This is especially true for retention times (RTs) >13 min, where TG and CE classes elute. The TIC for vendor 3 is much higher than both vendors 1 and 2 at RTs 13-16 min, with a substantially lower baseline at RTs >16 min. The low-mass region for each vendor was compared and *m/z* 102 is the most intense peak in each vendor solvents, however, a 13.3-fold reduction in *m/z* 102 is observed comparing vendors 2 and 1, and vendor 3 was found to have a 1.82-fold reduction in *m/z* 102 compared to vendor 1 (Supporting Figures S8 and S9). Comparing TG species, 1.64-fold and 2.84-fold increases in intensity were observed for TG 50:1, the most abundant TG species in the sample, when comparing vendor 1 solvents to vendors 2 and 3, respectively (Figure 4C). TG 48:0 experienced 1.87-fold and 3.46-fold increases in intensity in an analogous manner switching to solvents from vendors 2 and 3, respectively. Other abundant phospholipid classes, such as PC, PE, and LPC species, were not affected by vendor LCMS methanol and isopropanol selections (Figure 4D). Overall, vendor 3 had the greatest number of lipid annotations, with 344 total lipids, representing a 36% increase in annotations compared to using methanol and isopropanol from vendor 1 (Figure 4E). Despite vendor 2 having the lowest intensity impurity peaks, including *m/z* 102, in its low mass region, it did not produce the

highest number of lipid annotations, suggesting that other vendor-based contaminants or factors contribute to signal intensity.

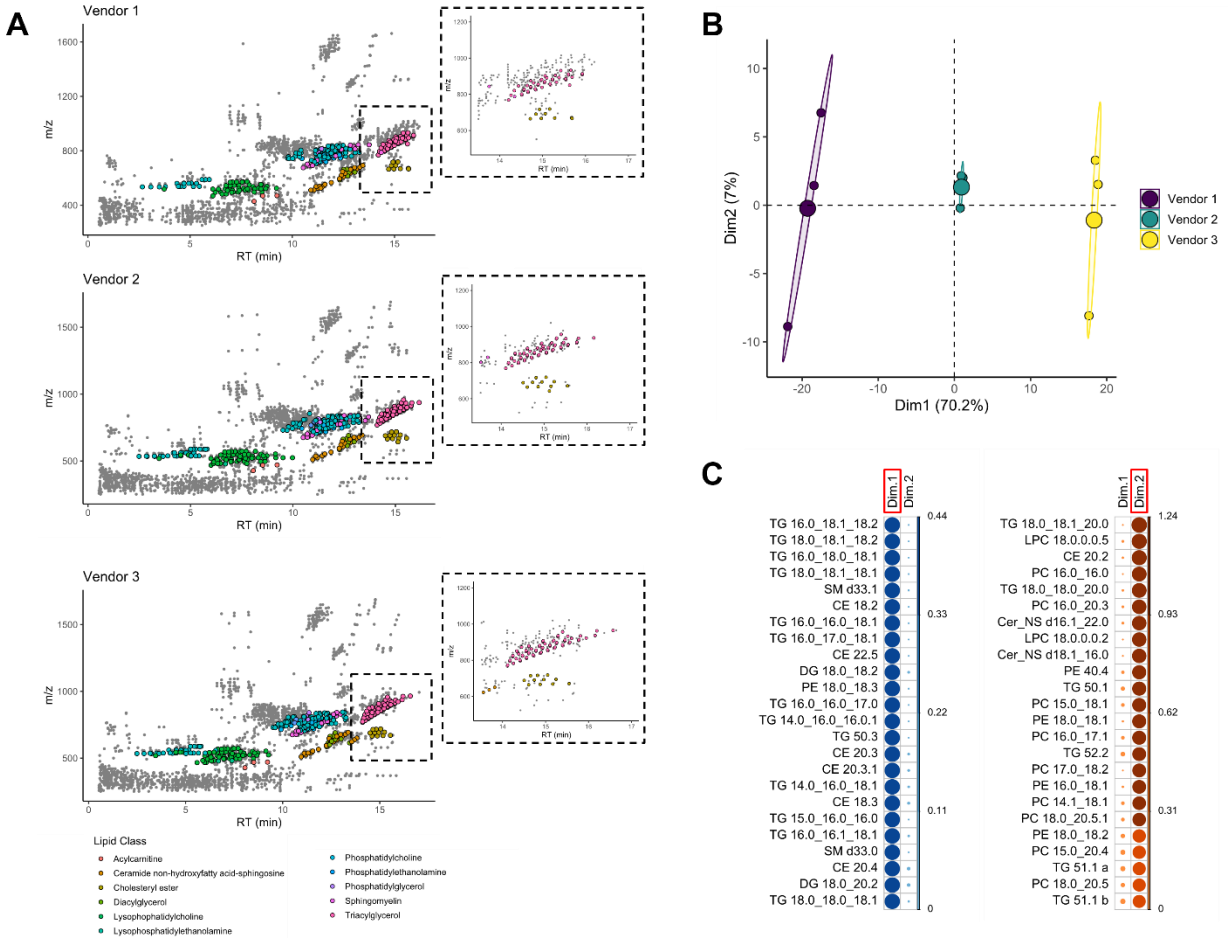

Figure 5. LCMS-grade methanol and isopropanol from different vendors have dramatic effects on the lipidomics dark matter that is observed in untargeted lipidomics studies. A) Scatter plots showing the dark matter in grey and annotated lipids coloured by class in the same sample of bovine liver extract analyzed with methanol and isopropanol from 3 different vendors. B) Principal component analysis (PCA) of the same bovine liver extract sample cluster separately from each other. C) Correlation plots showing the top 25 contributing lipids to Dim1 and Dim2 of the PCA in descending order.

To examine the differences that vendor solvent quality imparts on the lipidomics dark matter generated from the same sample, scatter plots showing all unknown and annotated features were produced (Figure 5A). Using the same Lipid Annotator method parameters, vendor 3 generated the most features (n=2319), while vendor 1 generated the fewest (n=2054). A complete list of features for each vendor can be found in a supporting Microsoft Excel worksheet containing the raw output from Lipid Annotator. This is especially observable for features with *m/z* <500, where vendor 3 had 838 features compared to 685 for vendor 1. CE and TG species simultaneously demonstrated a reduction in unknown features and an increase in lipid annotations when the solvents were switched from vendor 1 to either vendor 2 or vendor 3. The peak areas of annotated lipids were examined using principal component analysis (Figure 5B). All 3 vendors cluster separately, suggesting that sample reproducibility is highly dependent on LCMS solvent vendor choice. Dim1 of the PCA represents a large portion of the total variation between samples (70.2%). Correlation plots showing the contributions of the top 25 lipids contributing to Dim1 variation highlight the impact that neutral lipid species play in this variation, with 22 of the 25 lipids being from the TG, CE and DG classes. Dim2 represents dramatically less variation (7%) and is mostly made up of phospholipids and ceramide-containing species, likely highlighting the inter-replicate variation of the study. These results suggest that vendors of the same LCMS-grade solvents are optimally suited for certain applications, while being detrimental to others. For example, the methanol and isopropanol from vendor 1 have been shown in this study to be unsuitable for neutral lipid analysis; however, they appear to contain the least contaminant peaks overall, especially at lower RTs. As a result, vendor 1 solvents may be better suited for more polar

biomolecules, such as lyso lipid species or acylcarnitine focused applications. We therefore contend that solvent vendor selection, particularly in the case of methanol and isopropanol, should be carefully considered in method development and be a significant factor in the principle determinants of interlaboratory precision.

Conclusions

While researchers have focused on strategies to improve or expand characterization of the dark matter generated in lipidomics datasets, a great deal of work is still required to gain a comprehensive understanding of its origins. LCMS-grade solvent differences between vendors are often overlooked and have only recently been acknowledged to impact lipidomics studies. With the high-throughput capabilities and sensitivity of modern LCMS platforms, untargeted lipidomic applications generate thousands of features from a single sample. While ethylamine adducts have been previously reported to interfere with neutral lipid analysis and originate from acetonitrile, our results show that it is also a contaminant in a particular LCMS methanol and was not observed using acetonitrile. The results of this study show that a considerable portion of dark matter in some lipidomics datasets originates from spectral contamination caused by adduction of alkylated amine impurities found in LCMS solvents, shedding light onto a portion of the lipidomics dark matter that would not benefit from orthogonal separation techniques or novel informatics methods to elucidate its identity. Alkylated amine adducts represent a large number of meaningless spectral features that do not improve our understanding of the biological samples being analyzed, both wasting instrument time and reducing overall instrument sensitivity. Various efforts have been undertaken to bring standardization to the field of lipidomics, which is a major challenge considering the wide variability in protocols, instrument platforms and consumable products. We have demonstrated that large differences in lipidomics datasets can be directly attributed to LCMS methanol and isopropanol vendor selection. Vendor-based solvent differences can lead to dramatic variation in sensitivity that affect the analysis and ultimate results of entire

classes of neutral lipids. As a result, different LCMS-grade methanol and isopropanol products cannot be considered equivalent in their quality. Further complicating this situation, considerable variation in the total amounts of lipidomics dark matter is observed between vendors, increasing the enormity of the task of fully characterizing and understanding dark matter in lipidomics datasets. As a result, solvent vendor choice can have serious consequences to lipidomics experiments, requiring careful consideration during method development and data acquisition.

Associated Content:

The supporting information (SI) is available free of charge on the ACS Publications website at DOI: XXXX and contains additional chromatograms, diagrams, and tables, as referenced in the main article. A second Microsoft Excel worksheet is also included containing the Lipid Annotator output for a bovine liver extract sample analyzed using each vendor's solvents.

Author Information:

* Email: jeff.smith@carleton.ca Phone: +1 613-520-2600 ext. 2408

Author Contributions

J.A.R. was responsible for the experimental design. J.A.R., A.S.R., J.A.M., A.B., M.H. and K.V.W conducted the experimental work. K.V.W. was responsible for managing the laboratory environment. J.C.S. was responsible for funding the project and oversight of all activities. J.A.R. was responsible for writing the initial draft of the manuscript, A.S.R., J.A.M., J.M.M. and J.C.S. edited the manuscript, all co-authors reviewed and approved the final manuscript.

Notes

The authors declare no competing financial interests.

Acknowledgements:

J.C.S. and J.M.M. would like to gratefully acknowledge the Natural Sciences and Engineering Research Council of Canada, the Canada Foundation for Innovation, the Ontario Research Fund and Carleton University for research funding. J.A.R.

acknowledges the Ontario Graduate Scholarship program as well as Carleton University for internal scholarships. The authors graciously thank Prof. D. McMullin for access to an Agilent 1260 Infinity LC and 6230B TOF MS to confirm observations.

References

(1) Han, X.; Gross, R. W. The Foundations and Development of Lipidomics. *J. Lipid Res.* **2022**, *63* (2), 100164. https://doi.org/10.1016/J.JLR.2021.100164.

(2) Sud, M.; Fahy, E.; Cotter, D.; Brown, A.; Dennis, E. A.; Glass, C. K.; Merrill, A. H.; Murphy, R. C.; Raetz, C. R. H.; Russell, D. W.; Subramaniam, S. LMSD: LIPID MAPS Structure Database. *Nucleic Acids Res.* **2007**, *35* (suppl_1), D527–D532. https://doi.org/10.1093/NAR/GKL838.

(3) Conroy, M. J.; Andrews, R. M.; Andrews, S.; Cockayne, L.; Dennis, E. A.; Fahy, E.; Gaud, C.; Griffiths, W. J.; Jukes, G.; Kolchin, M.; Mendivelso, K.; Lopez-Clavijo, A. F.; Ready, C.; Subramaniam, S.; O, V. B. LIPID MAPS: Update to Databases and Tools for the Lipidomics Community. *Nucleic Acids Res.* **2023**, 1–6. https://doi.org/10.1093/nar/gkad896.

(4) Van Meer, G.; Voelker, D. R.; Feigenson, G. W. Membrane Lipids: Where They Are and How They Behave. *Nat. Rev. Mol. Cell Biol.* **2008**, *9* (2), 112–124. https://doi.org/10.1038/nrm2330.

(5) Olzmann, J. A.; Carvalho, P. Dynamics and Functions of Lipid Droplets. *Nat. Rev. Mol. Cell Biol.* **2019**, *20* (3), 137–155. https://doi.org/10.1038/s41580-018-0085-z.

(6) Blanksby, S. J.; Mitchell, T. W. Advances in Mass Spectrometry for Lipidomics. *Annu. Rev. Anal. Chem.* **2010**, *3* (1), 433–465. https://doi.org/10.1146/annurev.anchem.111808.073705.

(7) Chan, R. B.; Perotte, A. J.; Zhou, B.; Liong, C.; Shorr, E. J.; Marder, K. S.; Kang, U. J.; Waters, C. H.; Levy, O. A.; Xu, Y.; Shim, H. Bin; Pe'Er, I.; Di Paolo, G.; Alcalay, R. N. Elevated GM3 Plasma Concentration in Idiopathic Parkinson's Disease: A Lipidomic Analysis. *PLoS One* **2017**, *12* (2), e0172348–e0172348. https://doi.org/10.1371/journal.pone.0172348.

(8) Messias, M. C. F.; Mecatti, G. C.; Priolli, D. G.; De Oliveira Carvalho, P. Plasmalogen Lipids: Functional Mechanism and Their Involvement in Gastrointestinal Cancer. *Lipids in Health and Disease*. BioMed Central Ltd. March

7, 2018. https://doi.org/10.1186/s12944-018-0685-9.

(9) Proitsi, P.; Kim, M.; Whiley, L.; Simmons, A.; Sattlecker, M.; Velayudhan, L.; Lupton, M. K.; Soininen, H.; Kloszewska, I.; Mecocci, P.; Tsolaki, M.; Vellas, B.; Lovestone, S.; Powell, J. F.; Dobson, R. J. B.; Legido-Quigley, C. Association of Blood Lipids with Alzheimer's Disease: A Comprehensive Lipidomics Analysis. *Alzheimer's Dement.* **2017**, *13* (2), 140–151. https://doi.org/10.1016/j.jalz.2016.08.003.

(10) Monge, M. E.; Dodds, J. N.; Baker, E. S.; Edison, A. S.; Fernandez, F. M. Challenges in Identifying the Dark Molecules of Life. *Annu. Rev. Anal. Chem.* **2019**, *12*, 177–199. https://doi.org/10.1146/annurev-anchem-061318-114959.

(11) Skinner, O. S.; Kelleher, N. L. Illuminating the Dark Matter of Shotgun Proteomics. *Nat. Biotechnol.* **2015**, *33* (7), 717–718. https://doi.org/10.1038/nbt.3287.

(12) Da Silva, R. R.; Dorrestein, P. C.; Quinn, R. A. Illuminating the Dark Matter in Metabolomics. *Proc. Natl. Acad. Sci. U. S. A.* **2015**, *112* (41), 12549–12550. https://doi.org/10.1073/PNAS.1516878112/ASSET/FCB96DFB-4497-4C31-97E2-265AF95CF1E8/ASSETS/GRAPHIC/PNAS.1516878112FIG01.JPEG.

(13) Foster, M.; Rainey, M.; Watson, C.; Dodds, J. N.; Kirkwood, K. I.; Fernández, F. M.; Baker, E. S. Uncovering PFAS and Other Xenobiotics in the Dark Metabolome Using Ion Mobility Spectrometry, Mass Defect Analysis, and Machine Learning. *Environ. Sci. Technol* **2022**, *56*, 9133–9143. https://doi.org/10.1021/acs.est.2c00201.

(14) James, P. F.; Perugini, M. A.; O'Hair, R. A. J. Sources of Artefacts in the Electrospray Ionization Mass Spectra of Saturated Diacylglycerophosphocholines: From Condensed Phase Hydrolysis Reactions Through to Gas Phase Intercluster Reactions. *J. Am. Soc. Mass Spectrom.* **2006**, *17* (3), 384–394. https://doi.org/10.1016/J.JASMS.2005.11.009.

(15) Hu, C.; Luo, W.; Xu, J.; Han, X. Recognition and Avoidance of Ion Source-Generated Artifacts in Lipidomics Analysis. *Mass Spectrom. Rev.* **2022**, *41* (1),

15. https://doi.org/10.1002/MAS.21659.

(16) Cajka, T.; Hricko, J.; Rudl Kulhava, L.; Paucova, M.; Novakova, M.; Fiehn, O.; Kuda, O. Exploring the Impact of Organic Solvent Quality and Unusual Adduct Formation during LC-MS-Based Lipidomic Profiling. *Metabolites* **2023**, *13* (9), 966. https://doi.org/10.3390/metabo13090966.

(17) Gu, Z.; Jiyuan, M.; Zhao, X.; Wu, J.; Zhang, D. Reduction of Nitriles to Amines in Positive Ion Electrospray Ionization Mass Spectrometry. *Rapid Commun. Mass Spectrom.* **2006**, *20*, 2969–2972. https://doi.org/10.1002/rcm.

(18) Byrdwell, W. C.; Kotapati, H. K.; Goldschmidt, R. Fast Chromatography of Pulse Triacylglycerols. *JAOCS, J. Am. Oil Chem. Soc.* **2023**, *100* (1), 25–43. https://doi.org/10.1002/aocs.12665.

(19) Teshima, K.; Kondo, T.; Maeda, C.; Oda, T.; Hagimoto, T.; Tsukuda, R.; Yoshimura, Y. Application of 1-Alkylamines to a Liquid Chromatographic/Turbo Ionspray Tandem Mass Spectrometric Method for Quantifying Metabolites of a New Bone Anabolic Agent, TAK-778, in Human Serum. *J. Mass Spectrom.* **2002**, *37* (6), 631–638. https://doi.org/10.1002/jms.324.

(20) Mochida, Y.; Yokoyama, Y.; Nakamura, S. Effect of Amines of the Formation of Molecular Adduct Ions of Methyl Hydroperoxyoleates in Atmospheric Pressure Chemical Ionization Mass Spectrometry. *J. Mass Spectrom. Soc. Jpn.* **1998**, *46* (5), 454–458.

(21) Stefansson, M.; Sjöberg, P. J. R.; Markides, K. E. Regulation of Multimer Formation in Electrospray Mass Spectrometry. *Anal. Chem.* **1996**, *68* (10), 1792–1797. https://doi.org/10.1021/ac950980j.

(22) Bligh, E.G. and Dyer, W. J. Canadian Journal of Biochemistry and Physiology. *Can. J. Biochem. Physiol.* **1959**, *37* (8), 911–917.

(23) Whitehead, S. N.; Hou, W.; Ethier, M.; Smith, J. C.; Bourgeois, A.; Denis, R.; Bennett, S. A. L.; Figeys, D. Identification and Quantitation of Changes in the Platelet Activating Factor Family of Glycerophospholipids over the Course of

Neuronal Differentiation by High-Performance Liquid Chromatography Electrospray Ionization Tandem Mass Spectrometry. *Anal. Chem.* **2007**, *79* (22), 8539–8548. https://doi.org/10.1021/ac0712291.

(24) de Boer, J.; Backer, H. J. P-Tolylsulfonylmethylnitrosamide. *Org. Synth.* **1954**, *36*, 16.

(25) Wasslen, K. V.; Tan, L. H.; Manthorpe, J. M.; Smith, J. C. Trimethylation Enhancement Using Diazomethane (TrEnDi): Rapid on-Column Quaternization of Peptide Amino Groups via Reaction with Diazomethane Significantly Enhances Sensitivity in Mass Spectrometry Analyses via a Fixed, Permanent Positive Charge. *Anal. Chem.* **2014**, *86* (7), 3291–3299. https://doi.org/10.1021/AC403349C.

(26) Wasslen, K. V.; Canez, C. R.; Lee, H.; Manthorpe, J. M.; Smith, J. C. Trimethylation Enhancement Using Diazomethane (TrEnDi) II: Rapid in-Solution Concomitant Quaternization of Glycerophospholipid Amino Groups and Methylation of Phosphate Groups via Reaction with Diazomethane Significantly Enhances Sensitivity in Mass Spect. *Anal. Chem.* **2014**, *86* (19), 9523–9532. https://doi.org/10.1021/ac501588y.

(27) Chambers, M. C.; MacLean, B.; Burke, R.; Amodei, D.; Ruderman, D. L.; Neumann, S.; Gatto, L.; Fischer, B.; Pratt, B.; Egertson, J.; Hoff, K.; Kessner, D.; Tasman, N.; Shulman, N.; Frewen, B.; Baker, T. A.; Brusniak, M. Y.; Paulse, C.; Creasy, D.; Flashner, L.; Kani, K.; Moulding, C.; Seymour, S. L.; Nuwaysir, L. M.; Lefebvre, B.; Kuhlmann, F.; Roark, J.; Rainer, P.; Detlev, S.; Hemenway, T.; Huhmer, A.; Langridge, J.; Connolly, B.; Chadick, T.; Holly, K.; Eckels, J.; Deutsch, E. W.; Moritz, R. L.; Katz, J. E.; Agus, D. B.; MacCoss, M.; Tabb, D. L.; Mallick, P. A Cross-Platform Toolkit for Mass Spectrometry and Proteomics. *Nat. Biotechnol.* **2012**, *30* (10), 918–920. https://doi.org/10.1038/nbt.2377.

(28) Schmid, R.; Heuckeroth, S.; Korf, A.; Smirnov, A.; Myers, O.; Dyrlund, T. S.; Bushuiev, R.; Murray, K. J.; Hoffmann, N.; Lu, M.; Sarvepalli, A.; Zhang, Z.; Fleischauer, M.; Dührkop, K.; Wesner, M.; Hoogstra, S. J.; Rudt, E.; Mokshyna,

O.; Brungs, C.; Ponomarov, K.; Mutabdžija, L.; Damiani, T.; Pudney, C. J.; Earll, M.; Helmer, P. O.; Fallon, T. R.; Schulze, T.; Rivas-Ubach, A.; Bilbao, A.; Richter, H.; Nothias, L. F.; Wang, M.; Orešič, M.; Weng, J. K.; Böcker, S.; Jeibmann, A.; Hayen, H.; Karst, U.; Dorrestein, P. C.; Petras, D.; Du, X.; Pluskal, T. Integrative Analysis of Multimodal Mass Spectrometry Data in MZmine 3. *Nat. Biotechnol.* **2023**. https://doi.org/10.1038/s41587-023-01690-2.

(29) Hsu, F.; Turk, J. Energy Collisionally Activated Dissociation on a Triple Stage Quadrupole Instrument. *J. Am. Soc. Mass Spectrom.* **1999**, *10* (99), 600–612.

(30) Havrilla, C. M.; Hachey, D. L.; Porter, N. A. Coordination (Ag+) Ion Spray - Mass Spectrometry of Peroxidation Products of Cholesterol Linoleate and Cholesterol Arachidonate: High-Performance Liquid Chromatography - Mass Spectrometry Analysis of Peroxide Products from Polyunsaturated Lipid Autoxidati. *J. Am. Chem. Soc.* **2000**, *122* (33), 8042–8055. https://doi.org/10.1021/ja001180f.

(31) Schwudke, D.; Oegema, J.; Burton, L.; Entchev, E.; Hannich, J. T.; Ejsing, C. S.; Kurzchalia, T.; Shevchenko, A. Lipid Profiling by Multiple Precursor and Neutral Loss Scanning Driven by the Data-Dependent Acquisition. *Anal. Chem.* **2006**, *78* (2), 585–595. https://doi.org/10.1021/ac051605m.

(32) Cajka, T.; Fiehn, O. Increasing Lipidomic Coverage by Selecting Optimal Mobile-Phase Modifiers in LC–MS of Blood Plasma. *Metabolomics* **2016**, *12* (2), 1–11. https://doi.org/10.1007/s11306-015-0929-x.

(33) Shields, S. W. J.; Rosales, C. A.; Roberts, J. A.; Pallister, P. J.; Wasslen, K. V.; Manthorpe, J. M.; Smith, J. C. ITrEnDi: In Situ Trimethylation Enhancement Using Diazomethane: Improved and Expanded Glycerophospholipid and Sphingolipid Analyses via a Microscale Autonomous Derivatization Platform. *Anal. Chem.* **2021**, *93* (2), 1084–1091. https://doi.org/10.1021/acs.analchem.0c04088.

(34) Gonzalez-Riano, C.; Gradillas, A.; Barbas, C. Exploiting the Formation of Adducts in Mobile Phases with Ammonium Fluoride for the Enhancement of Annotation in Liquid Chromatography-High Resolution Mass Spectrometry Based Lipidomics. *J. Chromatogr. Open* **2021**, *1*. https://doi.org/10.1016/J.JCOA.2021.100018.

TOC Graphic – For table of contents use only